

Electronic Supplementary Information for

Highly Anisotropic Thermal Conductivity of Discotic Nematic Liquid Crystalline Films with Homeotropic Alignment

Dong-Gyun Kim,^{*ab} Yun Ho Kim,^{ab} Tae Joo Shin,^c Eun Jung Cha,^a Da Som Kim,^{ab}
Byoung Gak Kim,^{ab} Youngjae Yoo,^{ab} Yong Seok Kim,^{ab} Mi Hye Yi,^a and Jong Chan
Won^{ab}

^a Advanced Materials Division, Korea Research Institute of Chemical Technology, 141 Gajeong-ro, Yuseong-gu, Daejeon 34114, Republic of Korea.

^b Chemical Convergence Materials and Processes, University of Science and Technology, 217 Gajeong-ro, Yuseong-gu, Daejeon 34114, Republic of Korea.

^c UNIST Central Research Facilities & School of National Science, Ulsan National Institute of Science and Technology, 50 UNIST-gil, Eonyang-eup, Ulju-gun, Ulsan 44919, Republic of Korea.

**Corresponding author: D.-G. Kim (E-mail: dgkim@kriict.re.kr)*

Table of Contents

Materials	2
Synthesis of discotic nematic liquid crystals (DNLCs)	2
Preparation of DNLC films	3
Instrumentation and characterization techniques	3
Schematic illustration of 2D radial heat dissipation of h-DNLC film	6
Synthetic procedure and ¹ H NMR spectrum of DNLC 4	7
Thermal transition temperatures and POM images of DNLCs	8
Schematic illustration of DNLC film preparation	9
Optical observations of h-DNLC 2 and i-DNLC 4 film	10
2D WAXD analysis of DNLC films	11
Supplementary notes for thermal conductivity anisotropy of i-/a-DNLC 4 film	14
Thermal expansion analysis of DNLC films	16
References for electronic supplementary information	17

Materials

Ethyl 4-hydroxybenzoate (99%), 6-bromo-1-hexanol (97%), acryloyl chloride (97%), 1-bromodecane (98%), potassium carbonate (K_2CO_3 , $\geq 99\%$), hydrochloric acid (HCl, 37 wt% in H_2O), potassium hydroxide (KOH, 90%), sodium hydroxide (NaOH, 97%), triethylamine (TEA, $\geq 99\%$), methanesulfonyl chloride (MsCl, $\geq 99.7\%$), 1,2-dimethoxyethane (DME, anhydrous, 99.5%), 4-dimethylaminopyridine (DMAP, $\geq 99\%$), 4-methoxyphenol (MEHQ, 99%), all from Sigma-Aldrich, were used as received. Irgacure[®] 819 was purchased from BASF and used as received. 2,3,6,7,10,11-Hexahydroxytriphenylene (HHTP, hydrated, $>95\%$), obtained from HanChem, Co., Ltd. (Korea), was dried overnight under vacuum at 120 °C before use. 4-((6-(Acryloyloxy)hexyl)oxy)benzoic acid (ABA) and 4-(decyloxy)benzoic acid (DBA) were synthesized similarly to those described elsewhere.^{S1} All other reagents and solvents were used as received from standard vendors.

Synthesis of discotic nematic liquid crystals (DNLCs)

Discotic nematic liquid crystals (DNLCs) with ABA and DBA moieties were designated as DNLC #, where # is the average number of ABA moieties in the DNLC molecules. The following procedure was used for the synthesis of DNLC 4 containing average 4 ABA and average 2 DBA moieties. ABA (5.1 g, 17 mmol), DBA (2.4 g, 8.7 mmol), and DME (40 mL) were placed into a 250 mL round-bottomed flask with a magnetic stirring bar, then MsCl (2.0 mL, 26 mmol) and TEA (7.3 mL, 52 mmol) were added dropwise into the flask at 0 °C. After 2.5 h of stirring at room temperature, DMAP (0.43 g, 3.5 mmol) in DME (3.0 mL) was injected into the reaction flask at 0 °C, followed by the addition of HHTP (0.94 g, 2.9 mmol) in DME (7.0 mL). The mixture was allowed to react overnight at room temperature. After filtering the mixture to remove salts, the solution was diluted with 200 mL of methylene chloride (MC) and washed sequentially with 3M HCl and 3M NaOH aqueous solutions (200 mL each). The obtained organic layer was then dried over anhydrous $MgSO_4$ and concentrated under reduced pressure. The solution was precipitated into an excess of hexane, followed by reprecipitation into an excess of methanol to yield DNLC 4 (4.8 g, 85%). DNLCs of different composition were prepared using the same procedure, varying the

ratio of the ABA and DBA charges (Fig. S2). ^1H NMR of DNLC 4 (400 MHz, CDCl_3 , δ (ppm), TMS ref) (Fig. S3): 8.47 (s, 6H), 8.01 (m, 12H), 6.79 (m, 12 H), 6.40 (dd, 4H), 6.12 (dd, 4H), 5.81 (dd, 4H), 4.17 (t, 8H), 3.97 (t, 12H), 1.28 – 1.82 (m, 64H), 0.88 (t, 6H).

Preparation of DNLC films

A homogeneous mixture of DNLC 4 (0.11 g, with 200 ppm of MEHQ, an inhibitor to avoid thermal polymerization), Irgacure[®] 819 (1.1 mg, a photo-initiator), and acetone (1.0 mL) was cast on a glass substrate ($3.75 \times 3.75 \text{ cm}^2$) and the solvent was evaporated at room temperature for 1 h. After dried at $100 \text{ }^\circ\text{C}$ for 10 min, the solid mixture on glass substrate was heated to $140 \text{ }^\circ\text{C}$ to exhibit discotic nematic phase, which was then covered and pressed using another glass plate ($3.75 \times 3.75 \text{ cm}^2$). The gap between sandwiched glass plates was determined to be $65 \text{ }\mu\text{m}$, using a Kapton[®] tape as a spacer. Subsequently, photo-crosslinking of DNLCs was triggered by irradiating UV light (365 nm, 7.8 mW cm^{-1} , Blak-Ray[®], UVP) at $140 \text{ }^\circ\text{C}$ for 5 min. The two glass plates were carefully removed to give an as-prepared semi-transparent DNLC 4 film (a-DNLC 4). In order to prepare DNLC films with homeotropic alignment, an additional thermal treatment process was employed in between the cell assembly and the photo-crosslinking steps (Fig. S6). The DNLCs in the assembled cell was annealed at $200 \text{ }^\circ\text{C}$ (under its isotropic phase) for 1 min and cooled down to $140 \text{ }^\circ\text{C}$ at $5 \text{ }^\circ\text{C min}^{-1}$, followed by the photo-crosslinking. By using the thermal treatment process, transparent DNLC 4 and DNLC 2 films with homeotropic alignment were prepared and designated as h-DNLC 4 and h-DNLC 2, respectively. In addition, isotropic DNLC 4 film (i-DNLC 4) was also prepared by photo-crosslinking the DNLC 4 molecules at $200 \text{ }^\circ\text{C}$ for comparison purposes to study the effect of phase of DNLCs on thermal conductivity.

Instrumentation and characterization techniques

^1H NMR spectra of DNLCs were recorded on a Bruker Ascend 400 MHz using CDCl_3 , as a solvent. Differential scanning calorimetry (DSC) on DNLCs was run using a TA Instruments DSC Q200 under a nitrogen atmosphere. Samples with a typical mass of 5 – 10 mg were encapsulated in sealed aluminum pans. They were first heated from $40 \text{ }^\circ\text{C}$ to $200 \text{ }^\circ\text{C}$ and then cooled down to $0 \text{ }^\circ\text{C}$ at a constant rate of $5 \text{ }^\circ\text{C min}^{-1}$. Thermal

expansion tests on DNLC films were conducted using a TA instruments thermomechanical analyzer (TMA Q400). Rectangular specimens with a dimension of 8 mm in height, 4 mm in width, and 65 μm in thickness were used for the analysis. The measurements of thermal expansion of the films were made in the height direction, with an applied force of 0.05 N. The specimens were first heated from room temperature to 130 $^{\circ}\text{C}$ and then cooled down to 30 $^{\circ}\text{C}$ at a constant rate of 5 $^{\circ}\text{C min}^{-1}$ in a nitrogen atmosphere. Dimension change vs. temperature curves were obtained during the following 2nd heating step from 30 $^{\circ}\text{C}$ to 130 $^{\circ}\text{C}$ at a constant rate of 5 $^{\circ}\text{C min}^{-1}$. Polarized optical microscopy (POM) on DNLCs and DNLC films was performed using a Nikon Eclipse microscope (50i POL) coupled with a temperature controller (mK1000, INSTRON) at a heating and cooling rate of 5 $^{\circ}\text{C min}^{-1}$. Angular dependence of the birefringence of DNLC films was obtained using a Mueller matrix polarimeter (AxoScan[®], Axometrics). The 2D wide-angle X-ray diffraction (2D WAXD) measurements were carried at PLS-II 6D UNIST-PAL beamline of the Pohang Accelerator Laboratory in Korea. The synchrotron radiation coming from the bending magnets was monochromated using a Si(111) double crystal monochromator to deliver 11.6 keV (wavelength, $\lambda = 1.069 \text{ \AA}$) X-rays. The X-ray beam was focused both horizontally and vertically using the 2nd DCM crystal in sagittal shape and a toroidal focusing mirror to deliver 150 (H) x 120 (V) μm^2 (full-width at half maximum, FWHM) at the sample position. Thin film sample was mounted on the 4-axis precision goniometer equipped with two sets of high resolution CCD cameras. WAXD patterns were recorded with a 2D CCD detector (MX 225-HS, Rayonix L.L.C., USA) and diffraction angles were calibrated using a sucrose standard (Monoclinic, P2₁, a = 10.8631 \AA , b = 8.7044 \AA , c = 7.7624 \AA , $\beta = 102.938^{\circ}$). Thermal conductivity (κ) of DNLC films at room temperature was calculated as

$$\kappa = \alpha \times \rho \times C_p \quad (1)$$

where α is the thermal diffusivity ($\text{mm}^2 \text{ s}^{-1}$), ρ is the density (kg m^{-3}), and C_p is the specific heat capacity ($\text{J g}^{-1} \text{ K}^{-1}$) of the sample.^{S2} The thermal diffusivity (α) was measured at room temperature by laser flash analysis (LFA) method (LFA 447 NanoFlash[®], Netzsch). The method is compliant with the international standards ASTM E-1461, DIM EN 821, and DIN 30905. Circular samples with a dimension of 25.4

mm in diameter and 65 μm in thickness were used. At least three different samples were prepared for each DNLC film and tested in the LFA system. The density (ρ) was obtained by the equation, $\rho = m \times V^{-1}$, where the mass (m) was measured using electronic precision balance and the volume (V) was determined from the superficial area and thickness of the sample. The specific heat capacity (C_p) was measured by modulated differential scanning calorimetry (MDSC Q200, TA Instruments). Relative in-plane longitudinal and 2D radial heat transfer behaviors of DNLC films were observed by infrared (IR) camera (T300, FLIR). To place the DNLC films vertically on a hot plate for the in-plane longitudinal heat transfer imaging, a copper tape was attached to the end of rectangular-shaped samples with a dimension of 23 mm in length and 5 mm in width and fixed on the hot plate. After the hot plate was stabilized at 30 $^{\circ}\text{C}$, the setting temperature was raised to 100 $^{\circ}\text{C}$, and the heat flow along the longitudinal direction was traced over time. To image the 2D radial heat transfer of h-DNLC 4 film (circular shape, 25.4 mm in diameter), the film was placed on a 5 cm thick styrofoam panel which was equipped with a copper wire inside a narrowly punched hole. One end of the copper wire was fixed to the center of the film using a thermal paste and the other end was fixed to a hot plate. After the hot plate was stabilized at 30 $^{\circ}\text{C}$, the setting temperature was raised to 80 $^{\circ}\text{C}$, and the 2D radial heat flow was traced over time.

Schematic illustration of 2D radial heat dissipation of h-DNLC film

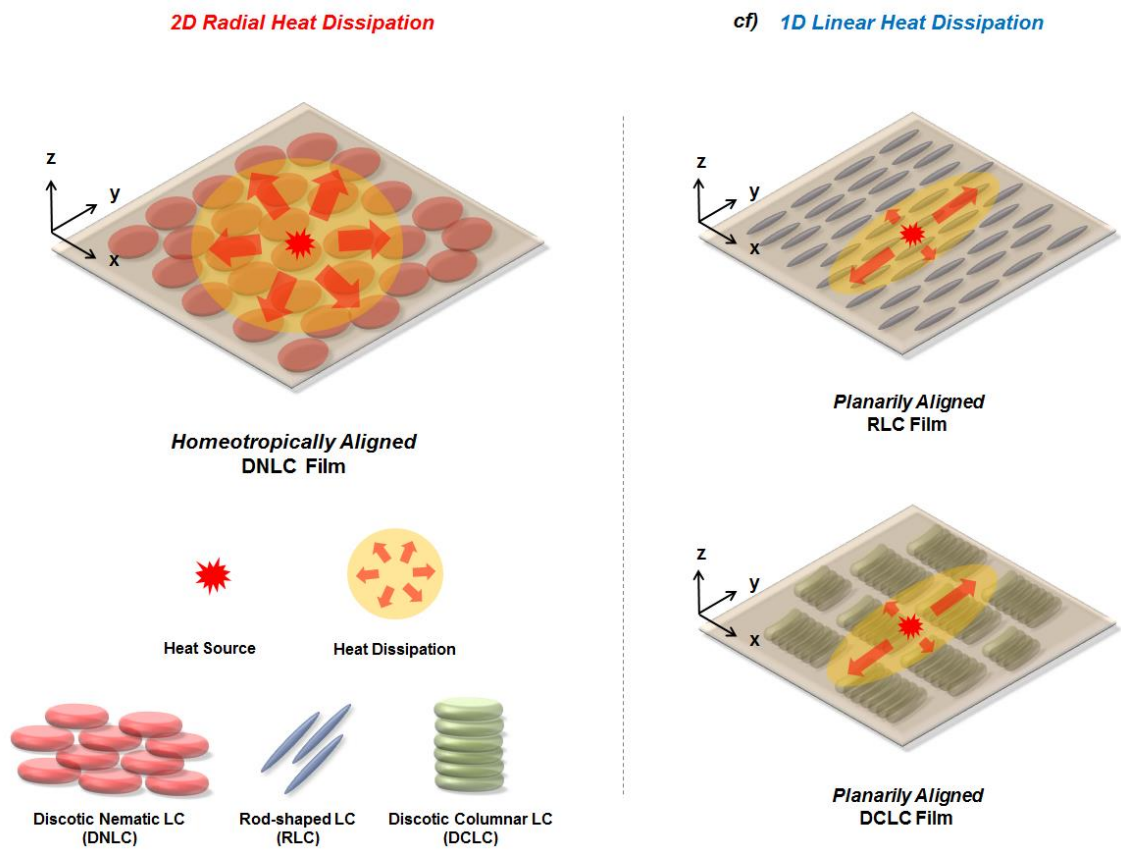


Fig. S1 Schematic illustration of 2D radial heat dissipation of a discotic nematic LC film with homeotropic alignment.

Synthetic procedure and ^1H NMR spectrum of DNLC 4

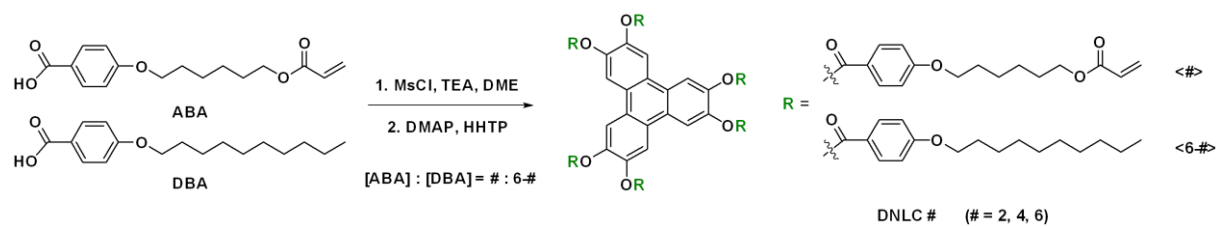


Fig. S2 Synthetic procedure of DNLCs. “ $\langle \# \rangle$ ” indicates the average number of ABA or DBA moieties in the DNLCs.

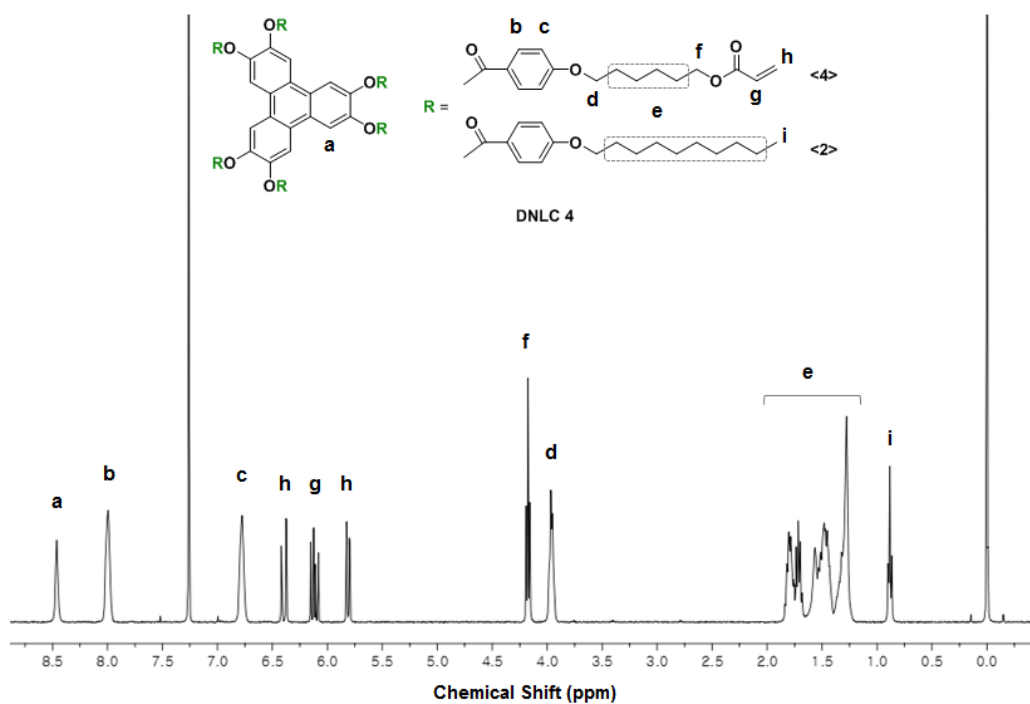


Fig. S3 ^1H NMR spectrum of DNLC 4.

Thermal transition temperatures and POM images of DNLCs

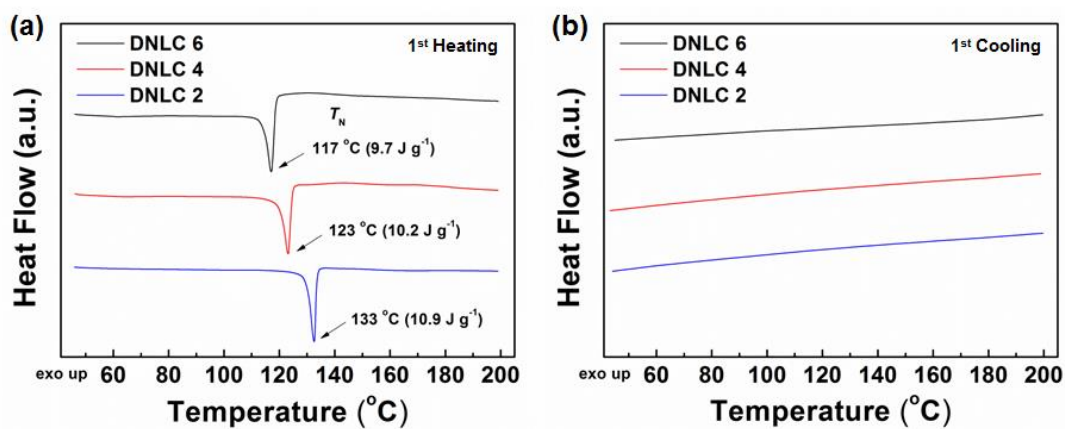


Fig. S4 (a) First heating and (b) cooling DSC thermograms of DNLCs obtained at a rate of 5 °C min⁻¹.

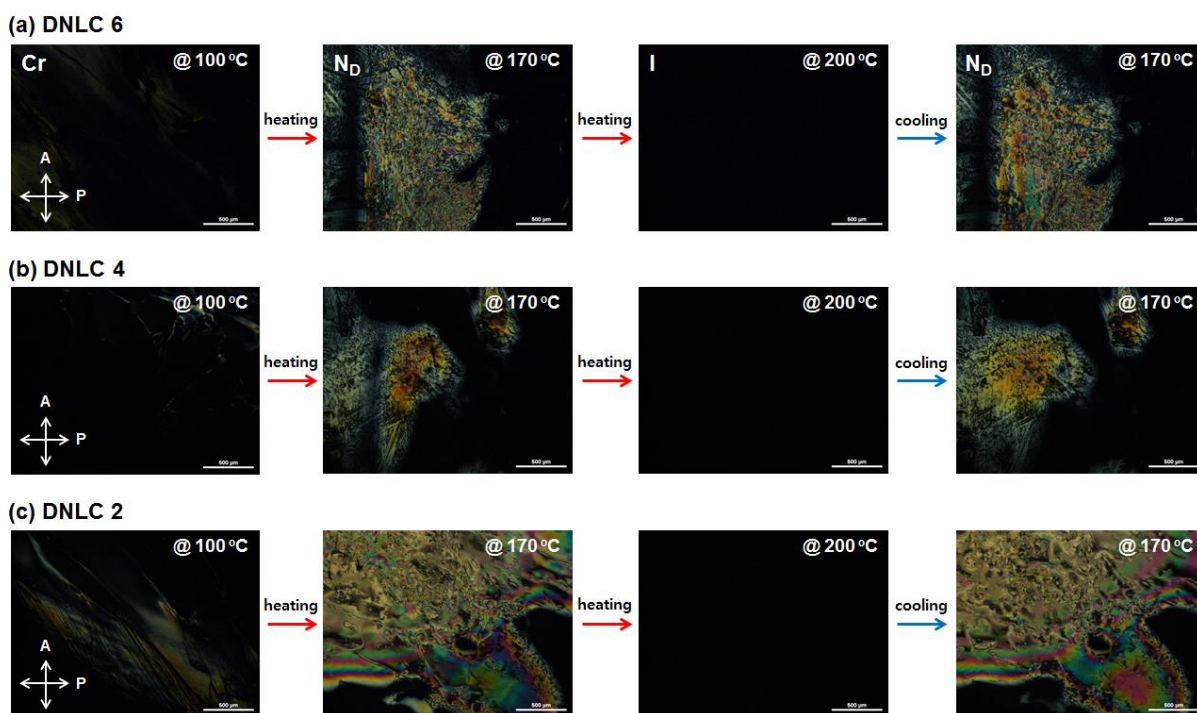


Fig. S5 POM images of DNLCs on glass substrate upon heating and cooling at 5 °C min⁻¹ (scale bar = 500 μm).

Schematic illustration of DNLC film preparation

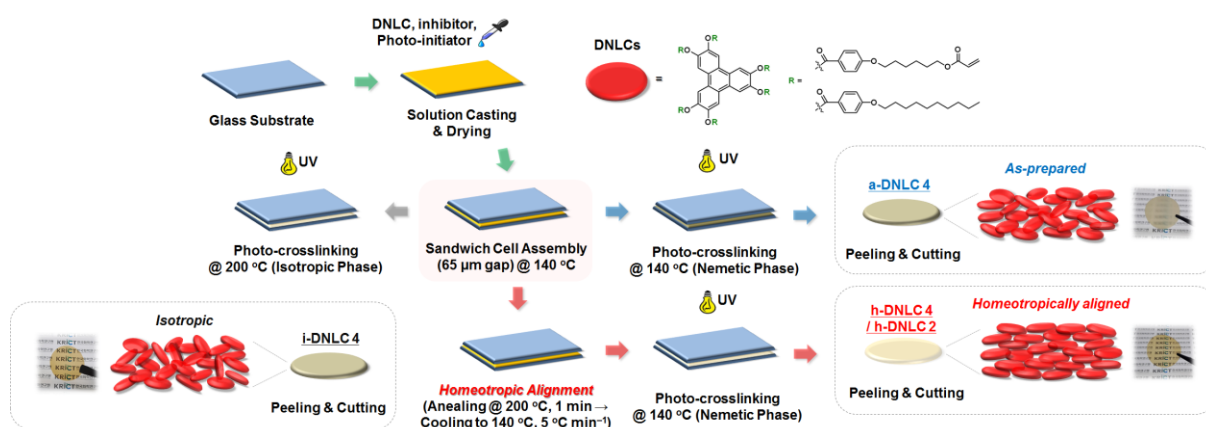


Fig. S6 Schematic illustration of fabrication procedure for DNLC films.

Triphenylene-based discotic liquid crystals with hydrophobic alkoxybenzoate arms, such as DNLCs in this study, can be oriented macroscopically on substrates *via* surface-induced molecular self-assembly.^{S3} Especially on substrates, such as hydrophilic glass, or those coated with polyvinyl alcohol- or acrylic acid-based alignment layers, DNLCs are known to exhibit a hybrid orientation, which possesses homeotropically oriented DNLCs near the substrate and obliquely oriented DNLCs with the hydrophobic arms stretching out to the air side near the free interface.^{S3} In order to achieve homeotropic orientation of DNLCs inside the whole film, some molecules, such as tris-dodecyloxylanilino-1,3,5-triazine, have been applied as homeotropic orientation accelerators, which can segregate in the interface between DNLCs and air to induce homeotropic orientation of DNLCs near the free interface.^{S3} In the present study, without using the homeotropic orientation accelerators, the air side of DNLCs on a glass substrate was simply covered using another glass substrate to provide confined hydrophilic interfaces, which was followed by the heat treatment and slow cooling process to provide enough mobility and time for homeotropic orientation of the DNLCs (Fig. S6).^{S4}

Optical observations of h-DNLC 2 and i-DNLC 4 films

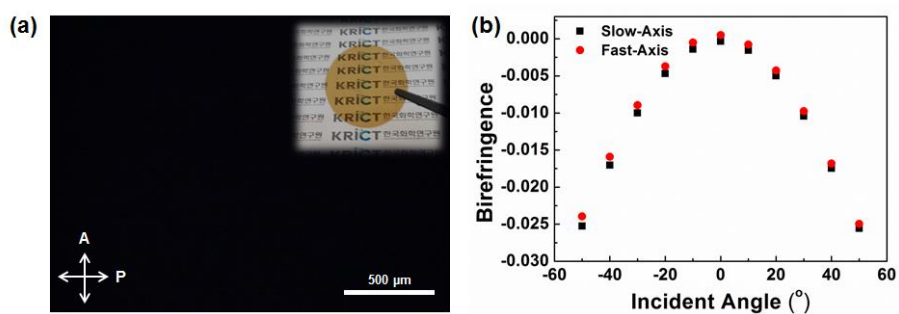


Fig. S7 (a) POM image and corresponding macroscopic image (inset) and (b) angular dependence of the birefringence of h-DNLC 2 film.

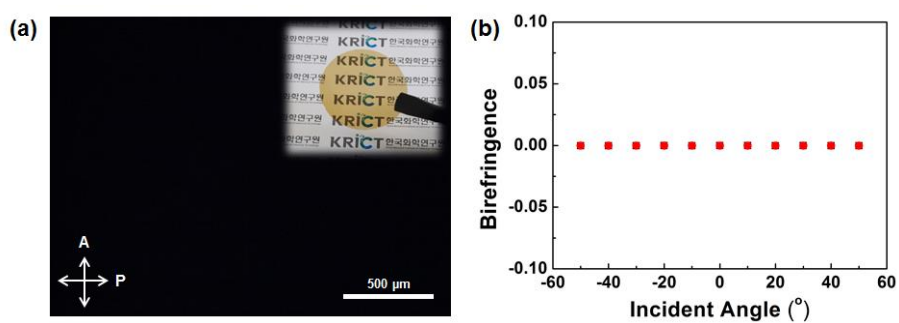


Fig. S8 (a) POM image and corresponding macroscopic image (inset) and (b) angular dependence of the birefringence of i-DNLC 4 film.

2D WAXD analysis of DNLC films

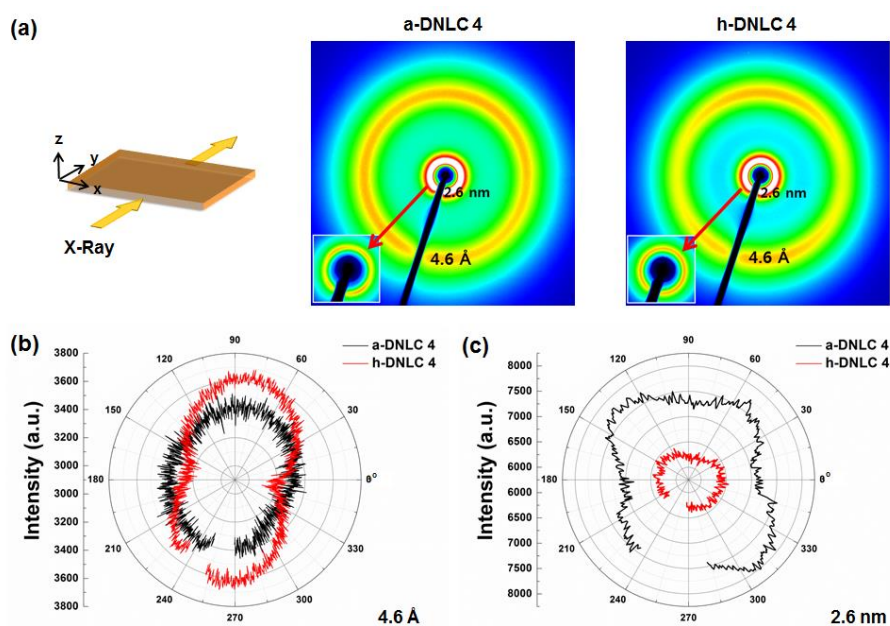


Fig. S9 (a) 2D WAXD patterns of a-DNLC₄ and h-DNLC₄ films and corresponding circular-cut profiles for (b) 4.6 Å and (c) 2.6 nm regions. The incident beam is parallel to the film surface. For the clarity, the enlarged 2.6 nm diffraction rings are displayed in insets with the different intensity scale.

Synchrotron 2D wide-angle X-ray diffraction (2D WAXD) technique was used to further investigate the DNLC alignments. Two distinct diffraction rings at $d = 2.6$ nm and 4.6 Å are clearly seen in the 2D WAXD patterns in Fig. S9a, which correspond to the diameter of possible DNLC columns and the average distance between stacked DNLC molecules, respectively.^{S5,S6} The 2D-WAXD pattern and circular-cut profile of h-DNLC₄ film in 4.6 Å, presenting azimuthal angle dependence of the intensity, show characteristic orientation of DNLC molecules (Fig. S9a and b). The larger intensities at 90° and 270° of h-DNLC₄ film than those at 0° and 180° suggest that the plane of DNLC₄ cores are oriented parallel to the film surface on average (*i.e.* homeotropic alignment),^{S5,S6} although the largest intensity axis is slightly tilted ($\sim 10^\circ$) from the 90°–270° axis. The asymmetric round-shaped circular-cut profile of a-DNLC₄ indicates that the a-DNLC₄ also has relatively larger content of DNLC₄ molecules oriented parallel to the film surface than those oriented vertical to the film surface, but its degree of asymmetry (*i.e.* degree of homeotropic alignment) is less than that of the h-

DNLC 4 film. The shear force applied in the direction parallel to the film surface during the sandwich cell assembly process as well as the geometric confinement by the sandwich glass cell could induce the asymmetric orientation of DNLC 4 molecules in the a-DNLC 4 film. In the circular-cut profile for 2.6 nm region, the h-DNLC 4 film shows an asymmetric circle with larger intensities in the direction of 0° - 180° axis, which is also in accord with the homeotropic alignment of the DNLCs. For the a-DNLC 4 film, relatively strong intensities are observed at 45° , 135° , 225° , and 315° of the circular-cut profile, suggesting the existence of columnar nematic phase tilted away from the plane of film surface at angles of $\pm 45^{\circ}$.^{S5,S6} As shown in Fig. S10, the circular-cut profiles of h-DNLC 2 film are close to those of h-DNLC 4 film, except greater overall intensities. This indicates that higher content of homeotropically aligned DNLC molecules are present in the h-DNLC 2 film, as compared with the h-DNLC 4 film. Although the 2D WAXD results could give some information on the relative homeotropic orientation of DNLC molecules, the overall homeotropic orientations do not seem to be very good. We attribute this to the intrinsically limited columnar stacking of DNLC molecules compared to the DCLCs. It has been reported that the orientation of DNLC core plane in the films is difficult to be observed clearly by 2D WAXD, due to the limited columnar stacking of DNLCs.^{S5-S8} This could make the detailed observation of subtle differences in DNLC orientations by the 2D WAXD difficult.

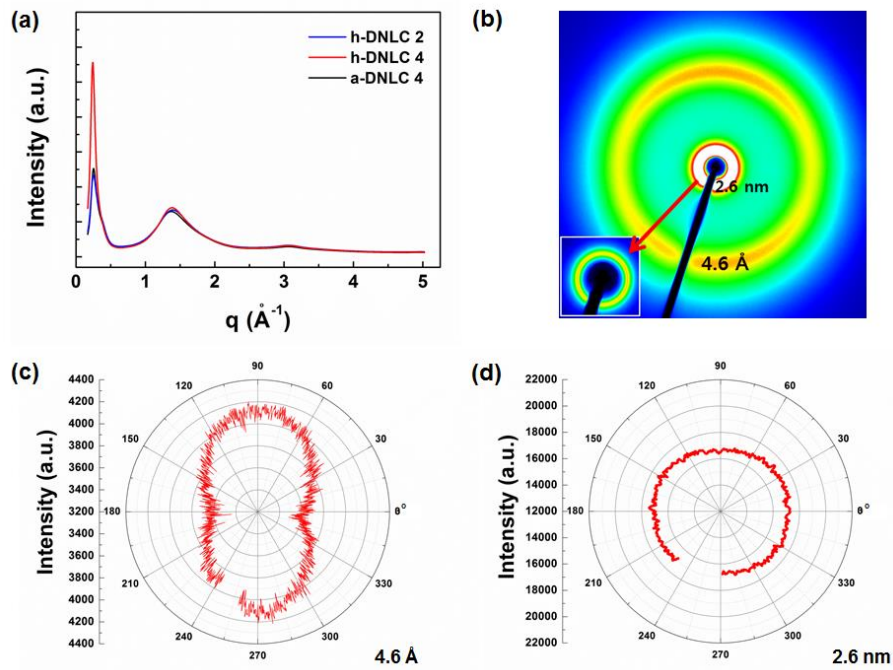


Fig. S10 (a) Averaged intensity vs. q plots for 2D WAXD of DNLC films. (b) 2D WAXD pattern of h-DNLC 2 film and corresponding circular-cut profiles for (c) 4.6 Å and (d) 2.6 nm regions. The incident beam is parallel to the film surface. For the clarity, the enlarged 2.6 nm diffraction rings are displayed in inset with the different intensity scale.

Supplementary notes for thermal conductivity anisotropy of i-/a-DNLC 4 films

In comparison to the bulk materials, thin films with thickness ranging from several nanometers to hundreds of microns are known to usually exhibit thickness-dependent and anisotropic thermal conductivities.^{S9-S13} Especially, the thermal conductivity of thin films can be strongly affected by the methods and substrates used for the thin film preparation.^{S9} For example, polyimide (PI) films frequently exhibit appreciable anisotropy in thermal conductivities, which originates from the mechanical shear-induced casting process inducing the PI chain orientation parallel to the film plane.^{S12,S13} The thermal conductivity anisotropy of the i-DNLC 4 (isotropic phase) and a-DNLC 4 (non-aligned discotic nematic phase) films could originate from the film preparation process using the sandwich glass cell in this study. As shown in Fig. S11a, the geometric confinement by the sandwich glass cell could induce homeotropic orientation of DNLC molecules very near the glass surface even at the isotropic phase,^{S14} which could possibly lead to the thermal conductivity anisotropy of the i-DNLC 4 film. For the a-DNLC 4 film, the shear force applied in the direction parallel to the film surface during the sandwich cell assembly process as well as the geometric confinement by the sandwich glass cell could induce the additional asymmetric orientation of DNLC 4 molecules in the film (Fig. S11b).^{S15} This additional shear force could be responsible for the higher thermal conductivity anisotropy of a-DNLC 4 film than the i-DNLC 4 film. Thus, the geometric path of the films can also affect the thermal conductivity. However, in this study, we used DNLC films with the same dimension for the thermal conductivity analysis, and the homeotropically aligned h-DNLC 4 film clearly exhibits much higher in-plane thermal conductivity and thermal conductivity anisotropy as compared with the non-aligned a-DNLC 4 film. Therefore, it can be concluded that the control of orientational direction of the DNLC molecules is a crucial factor for enabling DNLC-based TCIMs with strongly anisotropic thermal conductivity. Meanwhile, we believe that the thermal conductivity anisotropy of DNLC films could be affected by the film thickness, because the effect of the geometric confinement by sandwich glass cell and the shear force applied in the cell assembly step can be varied depending on the gap height of the sandwich cell. The detailed preparation and characterization of DNLC films with different geometric

dimensions will be the subject of additional studies in our group as a follow-up study of this Communication.

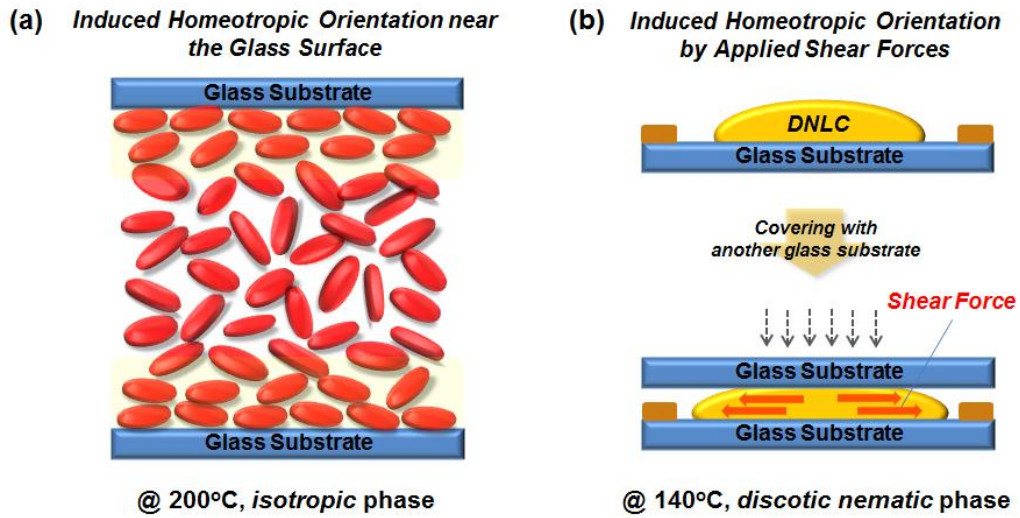


Fig. S11 Schematic illustrations of (a) induced homeotropic orientation of DNLCs near the glass surfaces at the isotropic phase and (b) induced homeotropic orientation by applied shear forces during the sandwich cell assembly process.

Thermal expansion analysis of DNLC films

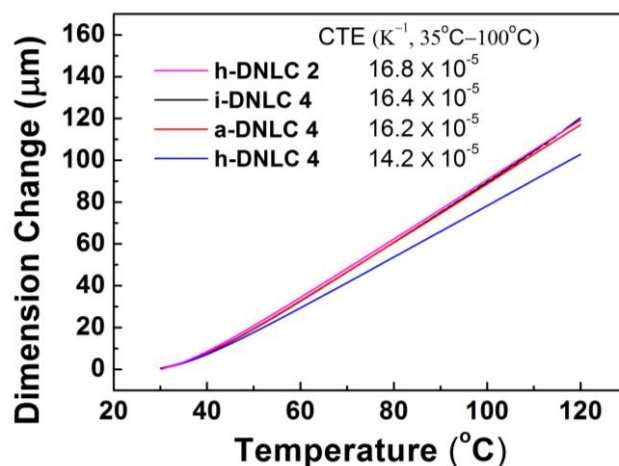


Fig. S12 Dimension change vs. temperature curves obtained from thermomechanical analysis (TMA) of DNLC films and corresponding coefficient of thermal expansion (CTE) values.

The CTE values of DNLC films in this study are found to be in the range of those of other polymer matrices of TCIMs ($6.5 \times 10^{-5} - 18.8 \times 10^{-5} K^{-1}$), such as poly(methyl methacrylate),^{S16} liquid crystalline polyesters,^{S17} polyamide,^{S18} and liquid crystalline epoxy polymers,^{S19} in the literature. Although it is difficult to compare the CTE values directly due to the different temperature ranges and experimental conditions for the CTE measurements, at least, such a comparison demonstrates that the DNLCs in this study can be applied as a polymeric matrix for TCIM applications. Meanwhile, the smallest CTE value of h-DNLC 4 among the DNLC films could be attributed to synergistic combination of the homeotropically ordered structure^{S20} and high crosslinking density^{S21} of DNLC 4 molecules in the films.

References for electronic supplementary information

- (S1) C. D. Favre-Nicolin and J. Lub, *Macromolecules*, 1996, **29**, 6143–6149.
- (S2) H. Chen, V. V. Ginzburg, J. Yang, Y. Yang, W. Liu, Y. Huang, L. Du and B. Chen, *Prog. Polym. Sci.*, 2016, **59**, 41–85.
- (S3) K. Kawata, *Chem. Rec.*, 2002, **2**, 59–80.
- (S4) M. Yoshio, T. Kagata, K. Hoshino, T. Mukai, H. Ohno and T. Kato, *J. Am. Chem. Soc.*, 2006, **128**, 5570–5577.
- (S5) C. D. Favre-Nicolin, J. Lub and P. V. D. Sluis, *Adv. Mater.*, 1996, **8**, 1005–1008.
- (S6) J. J. Ge, S.-C. Hong, B. Y. Tang, C. Y. Li, D. Zhang, F. Bai, B. Mansdorf, F. W. Harris, D. Yang, Y.-R. Shen and S. Z. D. Cheng, *Adv. Funct. Mater.*, 2003, **13**, 718–725.
- (S7) P. H. J. Kouwer, W. F. Jager, W. j. Mijs and S. J. Picken, *Macromolecules*, 2000, **33**, 4336–4342.
- (S8) J. H. Lee, I. Jang, S. H. Hwang, S. J. Lee, S. H. Yoo and J. Y. Jho, *Liq. Cryst.*, 2012, **39**, 973–981.
- (S9) D. Zhao, X. Qian, X. Gu, S. A. Jajja and R. Yang, *J. Electron. Packag.*, 2016, **138**, 040802–1–19.
- (S10) S. Lee and D. Kim, *Thermochim. Acta*, 2017, **653**, 126–132.
- (S11) N. Song, D. Jiao, S. Cui, X. Hou, P. Ding and L. Shi, *ACS Appl. Mater. Interfaces*, 2017, **9**, 2924–2932.
- (S12) M. Tanimoto, T. Yamagata, K. Miyata and S. Ando, *ACS Appl. Mater. Interfaces*, 2013, **5**, 4374–4382.
- (S13) K. Kurabayashi and K. E. Goodson, *J. Appl. Phys.*, 1999, **86**, 1925–1931.
- (S14) I. Abdulhalim, *J. Nanophotonics*, 2012, **6**, 061001–1–27.
- (S15) I. Soga, A. Dhinojwala and S. Granick, *Jpn. J. Appl. Phys.*, 1999, **38**, 6118–6122.
- (S16) C. Zhi, Y. Bando, C. Tang, H. Kuwahara and D. Golberg, *Adv. Mater.*, 2009, **21**, 2889–2893.
- (S17) S. M. Ha, H. L. Lee, S.-G. Lee, B. G. Kim, Y. S. Kim, J. C. Won, W. J. Choi, D. C. Lee, J. Kim and Y. Yoo, *Compos. Sci. Technol.*, 2013, **88**, 113–119.
- (S18) Y. Yoo, H. L. Lee, S. M. Ha, B. G. Kim, J. C. Won and S.-G. Lee, *Polym. Int.*, 2014, **63**, 151–157.
- (S19) Y.-S. Lin, S. L.-C. Hsu, T.-H. Ho, S.-S. Cheng and Y.-H. Hsiao, *Polym. Eng. Sci.*, 2017, **57**, 424–431.
- (S20) S. Ebisawa, J. Ishii, M. Sato, L. Vladimirov and M. Hasegawa, *Eur. Polym. J.*, 2010, **46**, 283–297.
- (S21) S. Yang and J. Qu, *Polymer*, 2012, **53**, 4806–4817.